Journal of Ocean Engineering and Marine Energy
https://doi.org/10.1007/s40722-024-00361-x

RESEARCH

Inverse non-linear problem of the long-wave run-up on coast

Alexei Rybkin[1] · Efim Pelinovsky[2,3] · Oleksandr Bobrovnikov[1] · Noah Palmer[4] · Ekaterina Pniushkova[5] · Daniel Abramowicz[6]

Received: 28 February 2024 / Accepted: 4 November 2024

Abstract

The study of the process of catastrophic tsunami-type waves on the coast makes it possible to determine the destructive force of waves on the coast. In hydrodynamics, the one-dimensional theory of the run-up of non-linear waves on a flat slope has gained great popularity, within which rigorous analytical results have been obtained in the class of non-breaking waves. In general, the result depends on the characteristics of the wave approaching (or generated on) the slope, which is usually not known in the measurements. Here, we describe a rigorous method for recovering the initial displacement in a source localised in an inclined power-shaped channel from the characteristics of a moving shoreline. The method uses the generalised Carrier–Greenspan transformation, which allows one-dimensional non-linear shallow-water equations to be reduced to linear ones. The solution is found in terms of Erdélyi–Kober integral operator. Numerical verification of our results is presented for the cases of a parabolic bay and an infinite plane beach.

1 Introduction

With the devastating loss of life caused by tsunamis such as the Indian Ocean Tsunami in 2004 and the Tōhoku Tsunami in 2011, predictive modelling of tsunami wave run-up is of great practical importance. In modern tsunami wave modelling, the shallow-water, or long-wave, approximations are commonly used to predict inundation areas (Levin and Nosov 2016). Such models require initial conditions to compute wave propagation. However, due to a lack of data on initial water displacement, models such as the Okada seismic model (Okada 1992) are often used to generate the initial data. An alternative approach is to indirectly estimate characteristics of the tsunami source through various inversion methods. Implementations have been used to recover the initial height of the water at the source (Abe 1973), the source location (Fujii et al. 2011), as well as fault motion (Satake 1987) to name just three. The latter, through the inversion of data gathered for the wave signal, is crucial in such fields as seismic hazard assessment. Through studying the accumulation of slip on each segment of a fault via the inverse problem, the prediction of earthquake recurrence intervals becomes increasingly more accurate. We suggest the recent review by Satake (2022) and the sources therein for more details on tsunami inversion methods, including waveform inversion, inverse modelling for the purpose of examining the tsunami source, and the generation of tsunami inverse refraction diagrams. Note that most methods assume that wave propagation is linear, while the tsunami wave run-up is a notoriously non-linear phenomenon. Unfortunately, inverse problems for non-linear PDEs are intractable in general. Thus, identifying

✉ Oleksandr Bobrovnikov
obobrovnikov@alaska.edu

Alexei Rybkin
arybkin@alaska.edu

Efim Pelinovsky
Pelinovsky@gmail.com

Noah Palmer
noah.palmer@colorado.edu

Ekaterina Pniushkova
katya.pniushkova@gmail.com

Daniel Abramowicz
dlabramowicz@dons.usfca.edu

1 Department of Mathematics and Statistics, University of Alaska Fairbanks, P O Box 756660, Fairbanks, AK 99775, USA

2 HSE University, Nizhny Novgorod, Russia

3 Institute of Applied Physics, Nizhny Novgorod, Russia

4 Department of Applied Mathematics, University of Colorado Boulder, Boulder, CO, USA

5 Department of Biomedical Engineering, Northwestern University, Evanston, IL, USA

6 Department of Mathematics, University of San Francisco, San Francisco, CA, USA

Published online: 22 November 2024

a realistic class of bathymetries where non-linear inversion methods can be applied is a primary objective of our research.

Currently, tsunami inundation calculations are conducted using numerical codes that model wave propagation from the source to the coast, validated against a series of benchmarks supported by experimental data. A significant part of this work involves analyzing the run-up of non-linear long waves on a flat slope, which has a rigorous analytical solution in the class of non-breaking waves using the Carrier–Greenspan transformation. The Carrier–Greenspan transformation simplifies the non-linear shallow-water equations to a linear wave equation with cylindrical symmetry (a particular class of the Euler–Poisson–Darboux equation) (Carrier and Greenspan 1958). Within this framework, the run-up of waves generated on the slope is considered, using various forms of initial displacement with the initial displacement of the water surface, such as solitons (Synolakis 1987), Gaussian (Carrier et al. 2003) and Lorentz (Pelinovsky and Mazova 1992) pulses, N-waves (Tadepalli and Synolakis 1994), cnoidal waves (Synolakis et al. 1988), algebraic pulses (Dobrokhotov et al. 2017), and the Okada solution (Tinti and Tonini 2005; Løvholt et al. 2012). Naturally, the specific characteristics of the run-up depend on the features of the initial displacement at the source. Thus, attempts have been made to parametrise these formulas to reduce the number of initial perturbation parameters (Didenkulova et al. 2008; Løvholt et al. 2012). More broadly, recent studies have also considered the fluid velocity at the source (Kânoğlu and Synolakis 2006; Rybkin 2019) and addressed boundary problems for waves approaching the coast (Antuono and Brocchini 2007; Aydin 2020). Similar approaches have also been developed for wave run-up in power-shaped bays (Hartle et al. 2021; Nicolsky et al. 2018; Rybkin et al. 2014, 2021; Shimozono 2016).

In the papers cited above, the direct problem (the Cauchy problem) of the non-linear equations of the shallow-water theory was solved. In this case, since there are no measurements of wave parameters in the shelf zone, model functions were used as initial conditions. In view of this, the inverse problem of recovering the initial conditions from the given (experimental or model) characteristics of the moving shoreline is of interest. This is especially important for fast estimates of tsunami waves in situations with uncertain wave properties during real events.

In this work, we consider the problem of recovering the shape of an incident wave from the known oscillations of a moving shoreline. This problem was first considered in Rybkin et al. (2023) and our work here is a generalisation of those results to a more diverse set of bathymetries. In this case, the following restrictions are imposed: the tsunami source is located on a slope at an arbitrary distance from the shoreline. Two configurations of the bottom relief are considered: a flat slope and an inclined parabolic channel. The solution of the inverse problem is found using the Abel transform in the class of non-breaking waves.

Our work here is organised as follows. In Sect. 2, we introduce the shallow-water framework our model is built upon. In Sect. 3, we give the statement of both the direct and inverse problem and introduce the Carrier–Greenspan hodograph transformation on which our method is based. We solve both the direct and inverse problems in Sect. 4 through the derivation of what we call the shoreline equation, an equation relating the mechanical energy of the wave at the shoreline and the initial wave profile. Section 5 discusses the recovery of certain characteristics of the initial wave. In Sect. 6, we give numerical verifications of our method. Finally, in Sect. 7, we give some concluding remarks and discuss some potential future directions.

2 Shallow water equations (SWE)

The shallow-water equations (SWE) are a set of non-linear, hyperbolic PDEs which are commonly used to model tsunami wave run-up. The 2+1 [that is the unknown functions are of two spatial variables x, y and the temporal variable t] SWE are a simplification of the Euler equations, a highly non-linear 3+1 (that is the unknown functions are of three spatial variables x, y, z and the temporal variable t) system. They can be derived with the truncation of Taylor expansions of non-linear terms and the assumptions of no vorticity, small vertical velocity, and small depth/wavelength and wave height/depth ratios. The 2+1 SWE can be further reduced to a 1+1 system [that is now the functions are of x and t only] by assuming that the bathymetry is centred along the x axis and is uniformly inclined. For the bathymetries we are concerned with here (see Fig. 1), power-shaped bays with y cross-section $|y|^m$, the non-linear SWE in non-dimensional units are given as

$$\begin{aligned} \partial_t \eta + u\,(1+\partial_x \eta) + \frac{m}{m+1}\,(x+\eta)\,\partial_x u = 0, \\ \partial_t u + u\partial_x u + \partial_x \eta = 0, \end{aligned} \tag{2.1}$$

where $u(x,t)$ is the depth averaged flow velocity over the corresponding cross-section, and $\eta(x,t)$ is the water displacement exceeding the unperturbed water level. The total perturbed water depth is given as $H(x,t) = h(x) + \eta(x,t)$ along the x axis, where $h(x)$ is the depth of the bay, and so, in dimensionless units, we simply have $h(x) = x$. Typically, the system seen in (2.1) is given in dimensional units. The substitution

$$\begin{aligned} &\widetilde{x} = (H_0/\alpha)x, \quad \widetilde{t} = \sqrt{H_0/g}\,t/\alpha, \quad \widetilde{\eta} = H_0\eta, \\ &\widetilde{u} = \sqrt{H_0 g}\,u, \end{aligned} \tag{2.2}$$

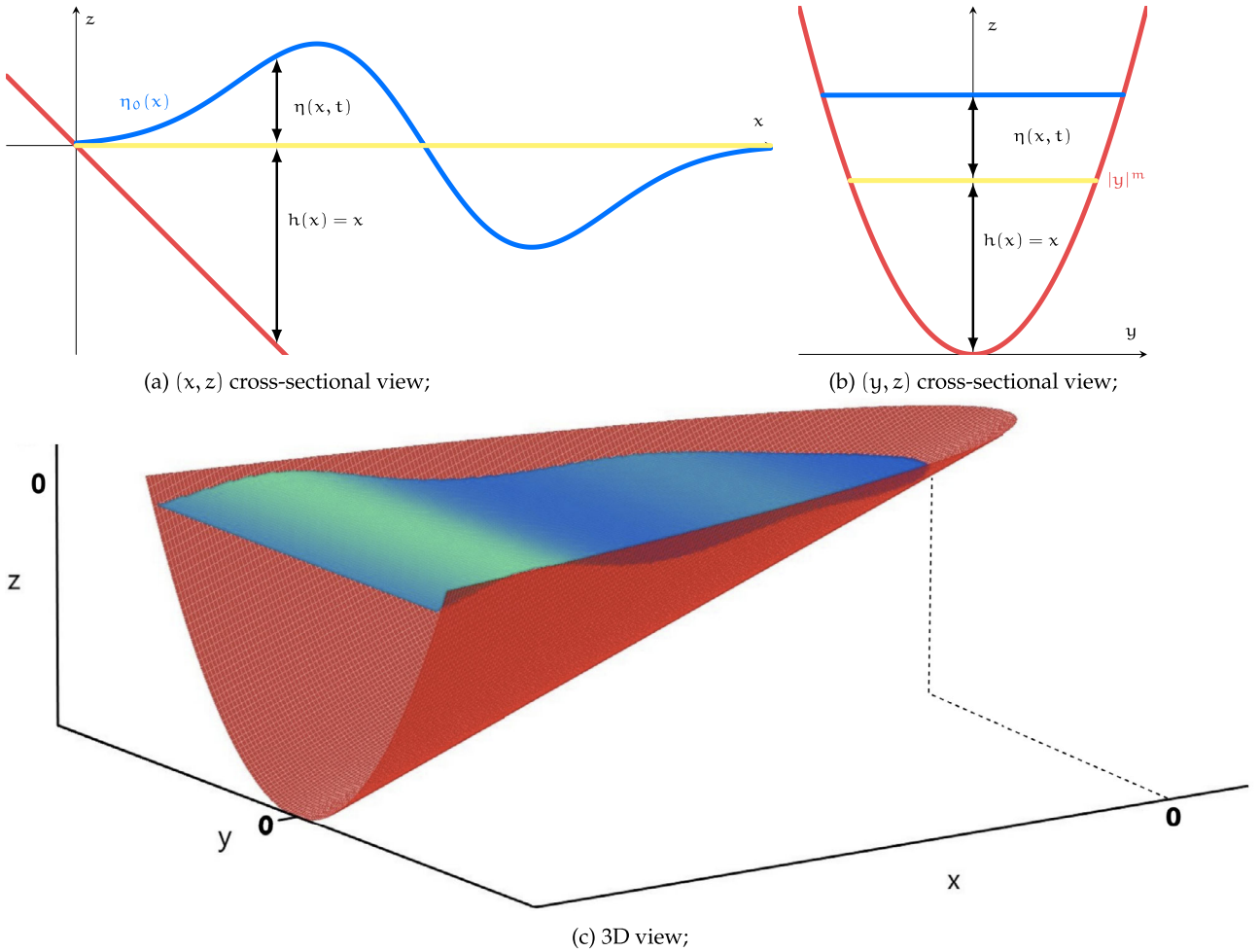

Fig. 1 Geometrical representations of a power-shaped bathymetry resembling the case $m = 2$. In 1a, we have cross sectional view of the xOz plane, in 1b a cross sectional view of the yOz plane, and in 1c a 3-dimensional view of the bay and an N-wave

where H_0 is the characteristic height of the wave, α is the slope of the bathymetry, and g is the acceleration of gravity, turns the dimensionless system into one with dimension (dimensional variables are the ones with tildes). The shoreline in the physical plane (i.e., the wet/dry boundary) is given by

$$x + \eta(x, t) = 0. \tag{2.3}$$

The solution to (2.3), let us call it $x_0(t)$, describes the run-up and draw-down of the tsunami wave. We consider the initial value problem for (2.1) with typical initial conditions characterised the instantaneous bottom displacement (see for instance Okada 1985)

$$\eta(x, 0) = \eta_0(x), \quad u(x, 0) = 0. \tag{2.4}$$

While the choice of zero initial velocity may be restrictive in physical application, there are good reasons for this choice. For earthquake generated tsunamis, it is typical to assume that the initial velocity is zero. Additionally, it is a convenient choice, a common technique in finding solutions to the SWE.

3 Statement of the direct and inverse problems

In this paper, we investigate the following direct problem: knowing the initial displacement of the water $\eta_0(x)$ and assuming zero initial velocity of the water, we find the movement of the shoreline $x_0(t)$. The direct problem was solved both numerically and analytically by many authors (see the references in the introduction). The corresponding inverse problem then consists of restoring the initial displacement of the water, assuming zero initial velocity and knowing the shoreline movement $x_0(t)$ and the time of an earthquake, i.e., zero time. It is worth noting that a non-linear inverse problem, as is the case with our problem, presents several challenges in terms of deriving a solution. The main difficulty is that

the shoreline is moving. The Carrier–Greenspan transform allows to reduce the original problem to a linear one on $\mathbb{R}_{>0}$.

Carrier–Greenspan Transform

The Carrier–Greenspan (CG) hodograph transform, introduced in Carrier and Greenspan (1958), can be used to linearise (2.1) into a form which can then be solved using Hankel transforms (Courant and Hilbert 1989). We use the form of the CG transform, originally introduced for power-shaped bays in Tuck and Hwang (1972)

$$\begin{aligned} &\varphi(\tau,\sigma) = u(x,t), \quad \sigma = x + \eta(x,t), \\ &\psi(\tau,\sigma) = \eta(x,t) + u^2(x,t)/2, \quad \tau = t - u(x,t). \end{aligned} \tag{3.1}$$

Applying (3.1) to (2.1) yields the linear hyperbolic system

$$\begin{aligned} \partial_\tau \psi + \frac{m}{m+1}\sigma\partial_\sigma\varphi + \varphi = 0, \\ \partial_\tau\varphi + \partial_\sigma\psi = 0, \end{aligned} \tag{3.2}$$

which is often written as the second-order equation

$$\partial_\tau^2\psi = \frac{m}{m+1}\sigma\partial_\sigma^2\psi + \partial_\sigma\psi. \tag{3.3}$$

We therefore obtain a linear hyperbolic equation (3.3) from a non-linear system (2.1). Physically, σ denotes wave height from the bottom, τ is a delayed time, φ is the flow velocity, and ψ can be called the total energy. The CG transforms main benefit is that the moving shoreline $x_0(t)$ is fixed at $\sigma = 0$. Nevertheless, the CG transform has some notable drawbacks; for one, the ICs become complicated in the hodograph coordinates, making standard techniques difficult to apply. However, by setting the initial velocity of the wave to be zero, that is $u_0(x) = 0$, one avoids this issue. While, this premiss is restrictive, it is typical when considering earthquake generated tsunamis. Thus, we assume this condition which is equivalent to $\varphi(0,\sigma) = 0$, and so, (2.4) becomes

$$\varphi\Big|_\Gamma = 0, \quad \psi\Big|_\Gamma = \psi_0(\sigma) = \eta_0(\gamma(\sigma)), \tag{3.4}$$

where Γ is the vertical line $(0,\sigma)$ in the hodograph plane and $x = \gamma(\sigma)$ solves $\sigma = \eta(x,t) + x$. Additionally, the regular singularity at $\sigma = 0$ causes computational difficulties at the shoreline. Finally, we note that the transformation only works provided that it is invertible, i.e., the wave does not break (Rybkin et al. 2021), so we must surmise this going forward.

4 The shoreline equation

In this section, we derive what we call the shoreline equation of an arbitrary power-shaped bay. Specifically, we derive an equation relating $\psi(\tau,0)$, the energy of the water at the shoreline, and $\psi(0,\sigma) = \psi_0(\sigma)$ the initial displacement of the water. Notably, the direct problem has previously been solved for power-shaped bathymetries (see, for instance, Garayshin et al. (2016); Didenkulova and Pelinovsky (2011)) and the inverse problem in the narrow case of a plane beach (Rybkin et al. 2023). Here, the direct problem is solved both analytically, as follows in this section, and numerically, as can be seen in Sect. 6, to ensure that propagation of the wave is being accounted for as described in Satake (1987). Since the energy at the shoreline can be computed from the movement of the shoreline $x_0(t)$, the shoreline equation allows us to easily solve the inverse problem and recover $\eta_0(x)$ after converting back into physical space.

We start with the bounded analytical solution to the initial value problem (3.3, 3.4), which is given in Rybkin et al. (2021)

$$\begin{aligned} \psi(\tau,\sigma) = \sigma^{-\frac{1}{2m}} \int_0^\infty 2k \left(\int_0^\infty \psi_0(s) s^{\frac{1}{2m}} J_{\frac{1}{m}}(2k\sqrt{s})\,\mathrm{d}s \right) \\ \cos\left(\sqrt{\frac{m}{m+1}}k\tau\right) J_{\frac{1}{m}}(2k\sqrt{\sigma})\,\mathrm{d}k, \end{aligned} \tag{4.1}$$

where $J_{\frac{1}{m}}$ is the Bessel function of the first kind of order $1/m$ and $\Gamma(z)$ is the gamma function. Since $J_\nu(z) = z^\nu 2^{-\nu}/\Gamma(\nu+1) + o(1)$ as $z \to +0$, we obtain

$$\begin{aligned} \psi(\tau,0) = \frac{2}{\Gamma(\frac{1}{m}+1)} \int_0^\infty k^{\frac{1}{m}+1} \\ \times \left(\int_0^\infty \psi_0(s) s^{\frac{1}{2m}} J_{\frac{1}{m}}(2k\sqrt{s})\,\mathrm{d}s \right) \\ \times \cos\left(\sqrt{\frac{m}{m+1}}k\tau\right)\mathrm{d}k, \end{aligned} \tag{4.2}$$

which after the substitution $\lambda = \sqrt{s}$ and $\widehat{\psi}_0(\lambda) = \psi_0(\lambda^2)$ becomes

$$\begin{aligned} \psi(\tau,0) = \frac{4}{\Gamma(\frac{1}{m}+1)} \int_0^\infty k^{\frac{1}{m}+1} \\ \times \left(\int_0^\infty \widehat{\psi}_0(\lambda) \lambda^{\frac{1}{m}+1} J_{\frac{1}{m}}(2k\lambda)\,\mathrm{d}\lambda \right) \\ \times \cos\left(\sqrt{\frac{m}{m+1}}k\tau\right)\mathrm{d}k. \end{aligned} \tag{4.3}$$

Now, define the modified Hankel transform as

$$\left[\widehat{\mathcal{H}}_\nu f(r)\right](k) = k^{-\nu} \int_0^\infty f(r) J_\nu(kr) r^{\nu+1}\,\mathrm{d}r. \tag{4.4}$$

Note that

$$\left[\widehat{\mathcal{H}}_\nu f(r)\right](\lambda) = \lambda^{-\nu}\left[\mathcal{H}_\nu r^\nu f(r)\right](\lambda), \tag{4.5}$$

where $\mathcal{H}_\nu$ is the standard Hankel transform, and so, we observe that $\widehat{\mathcal{H}}_\nu$ is self-inverse.

Therefore, applying (4.4) to (4.3), we have

$$\begin{aligned}\psi(\tau,0) &= \frac{2^{2+\frac{1}{m}}}{\Gamma(\frac{1}{m}+1)}\int_0^\infty k^{1+\frac{2}{m}}\left[\widehat{\mathcal{H}}_{\frac{1}{m}}\widehat{\psi}_0(\lambda)\right](2k)\\ &\quad\times\cos(2\pi\xi k)\,\mathrm{d}k,\end{aligned}\tag{4.6}$$

where $\xi = (\sqrt{m/(m+1)}\tau)/2\pi =: q^{-1}\tau$. Let $g(k) = k^{1+\frac{1}{2m}}\left[\widehat{\mathcal{H}}_{\frac{1}{m}}\widehat{\psi}_0(\lambda)\right](2k)$ and denote

$$[\mathcal{F}_c f(t)](\xi) = \int_0^\infty f(t)\cos(2\pi\xi t)\,\mathrm{d}t,\tag{4.7}$$

as the Fourier cosine transform. Then, we obtain

$$\begin{aligned}\psi(\tau,0) &= \frac{2^{2+\frac{1}{m}}}{\Gamma(\frac{1}{m}+1)}\int_0^\infty g(k)\cos(2\pi\xi k)\,\mathrm{d}k\\ &= \frac{2^{2+\frac{1}{m}}}{\Gamma(\frac{1}{m}+1)}[\mathcal{F}_c g(k)](\xi)\\ &= \frac{2^{2+\frac{1}{m}}}{\Gamma(\frac{1}{m}+1)}\left[\mathcal{F}_c k^{1+\frac{1}{2m}}\left[\widehat{\mathcal{H}}_{\frac{1}{m}}\widehat{\psi}_0(\lambda)\right](2k)\right](\xi).\end{aligned}\tag{4.8}$$

Therefore, (4.8) allows us to solve the direct problem. For that, one would need to find $\psi_0(\sigma)$ from the Carrier–Greenspan transform as

$$\eta_0(x) = \psi_0(\sigma), \quad \sigma = x + \eta_0(x),\tag{4.9}$$

then compute two integral transforms, and finally return to the (x,t) space using the inverse CG transform, which at the shoreline becomes

$$\psi(\tau,0) = -x_0(t) + \dot{x}_0(t)^2/2, \quad \tau = t - \dot{x}_0(t).\tag{4.10}$$

Solution to the inverse problem

In this section, we invert the transform given in (4.8) to solve the inverse problem.

Applying the inverse Fourier cosine transform to (4.8), we obtain

$$\begin{aligned}\frac{\Gamma(\frac{1}{m}+1)}{2^{2+\frac{1}{m}}}\psi(q\xi,0) &= [\mathcal{F}_c g(k)](\xi)\\ \frac{\Gamma(\frac{1}{m}+1)}{2^{2+\frac{1}{m}}}\left[\mathcal{F}_c^{-1}\psi(q\xi,0)\right](k) &= k^{1+\frac{1}{2m}}\left[\widehat{\mathcal{H}}_{\frac{1}{m}}\widehat{\psi}_0(\lambda)\right](2k)\\ \frac{\Gamma(\frac{1}{m}+1)}{2^{2+\frac{1}{m}}k^{1+\frac{1}{2m}}}\left[\mathcal{F}_c^{-1}\psi(q\xi,0)\right](k) &= \left[\widehat{\mathcal{H}}_{\frac{1}{m}}\widehat{\psi}_0(\lambda)\right](2k).\end{aligned}\tag{4.11}$$

Applying the inverse Hankel transform and utilising the identity (Gradshteyn and Ryzhik 2007)

$$\begin{aligned}J_\nu(z) &= \frac{2\left(\frac{z}{2}\right)^\nu}{\Gamma\left(\nu+\frac{1}{2}\right)\sqrt{\pi}}\int_0^1\cos zs(1-s^2)^{\nu-\frac{1}{2}}\,\mathrm{d}s\\ &\quad\text{for } z>0,\ \nu>-\frac{1}{2},\end{aligned}\tag{4.12}$$

we obtain

$$\begin{aligned}\widehat{\psi}_0(\lambda) &= 2\Gamma(1+1/m)\lambda^{-\frac{1}{m}}\\ &\quad\int_0^\infty\psi(q\xi,0)\cos(2\pi k\xi)\,\mathrm{d}\xi\,J_{\frac{1}{m}}(2k\lambda)\,\mathrm{d}(2k)\\ &\quad\text{[use integral representation of Bessel function]}\\ &= 2\Gamma\left(1+\frac{1}{m}\right)\lambda^{-\frac{1}{m}}\int_0^\infty k^{-\frac{1}{m}}\\ &\quad\int_0^\infty\psi(q\xi,0)\cos(2\pi k\xi)\,\mathrm{d}\xi\,\frac{2(k\lambda)^{\frac{1}{m}}}{\Gamma\left(\frac{1}{m}+\frac{1}{2}\right)\sqrt{\pi}}\\ &\quad\int_0^1\cos(2k\lambda s)(1-s^2)^{\frac{1}{m}-\frac{1}{2}}\,\mathrm{d}s\,\mathrm{d}(2k)\\ &\quad\text{[regroup and change order of integration]}\\ &= \frac{8\Gamma(1+1/m)}{\Gamma(1/m+1/2)\sqrt{\pi}}\int_0^1(1-s^2)^{\frac{1}{m}-\frac{1}{2}}\\ &\quad\int_0^\infty\int_0^\infty\cos(2\pi k\xi)\cos(2k\lambda s)\psi(q\xi,0)\,\mathrm{d}\xi\,\mathrm{d}k\,ds.\end{aligned}\tag{4.13}$$

Further change of variables $r = \lambda s/\pi$ yields

$$\begin{aligned}\widehat{\psi}_0(\lambda) &= \frac{8\Gamma(1+1/m)}{\Gamma(1/m+1/2)\sqrt{\pi}}\int_0^{\lambda/\pi}\left(1-\frac{\pi^2r^2}{\lambda^2}\right)^{\frac{1}{m}-\frac{1}{2}}\\ &\quad\int_0^\infty\int_0^\infty\cos(2\pi k\xi)\cos(2\pi kr)\psi(q\xi,0)\frac{\pi}{\lambda}\,\mathrm{d}\xi\,\mathrm{d}k\,\mathrm{d}r\\ &\quad\text{[split 8 = 2 · 4 and regroup]}\\ &= \frac{2\sqrt{\pi}\Gamma(1+1/m)}{\lambda\Gamma(1/m+1/2)}\int_0^{\lambda/\pi}\left(1-\frac{\pi^2r^2}{\lambda^2}\right)^{\frac{1}{m}-\frac{1}{2}}\\ &\quad 4\int_0^\infty\int_0^\infty\cos(2\pi k\xi)\cos(2\pi kr)\psi(q\xi,0)\,\mathrm{d}\xi\,\mathrm{d}k\,\mathrm{d}r\\ &\quad\text{[Fourier transforms cancel]}\\ &= \frac{2\sqrt{\pi}\Gamma(1+1/m)}{\lambda\Gamma(1/m+1/2)}\int_0^{\lambda/\pi}\left(1-\left(\frac{\pi r}{\lambda}\right)^2\right)^{1/m-1/2}\\ &\quad\psi(qr,0)\,\mathrm{d}r.\end{aligned}\tag{4.14}$$

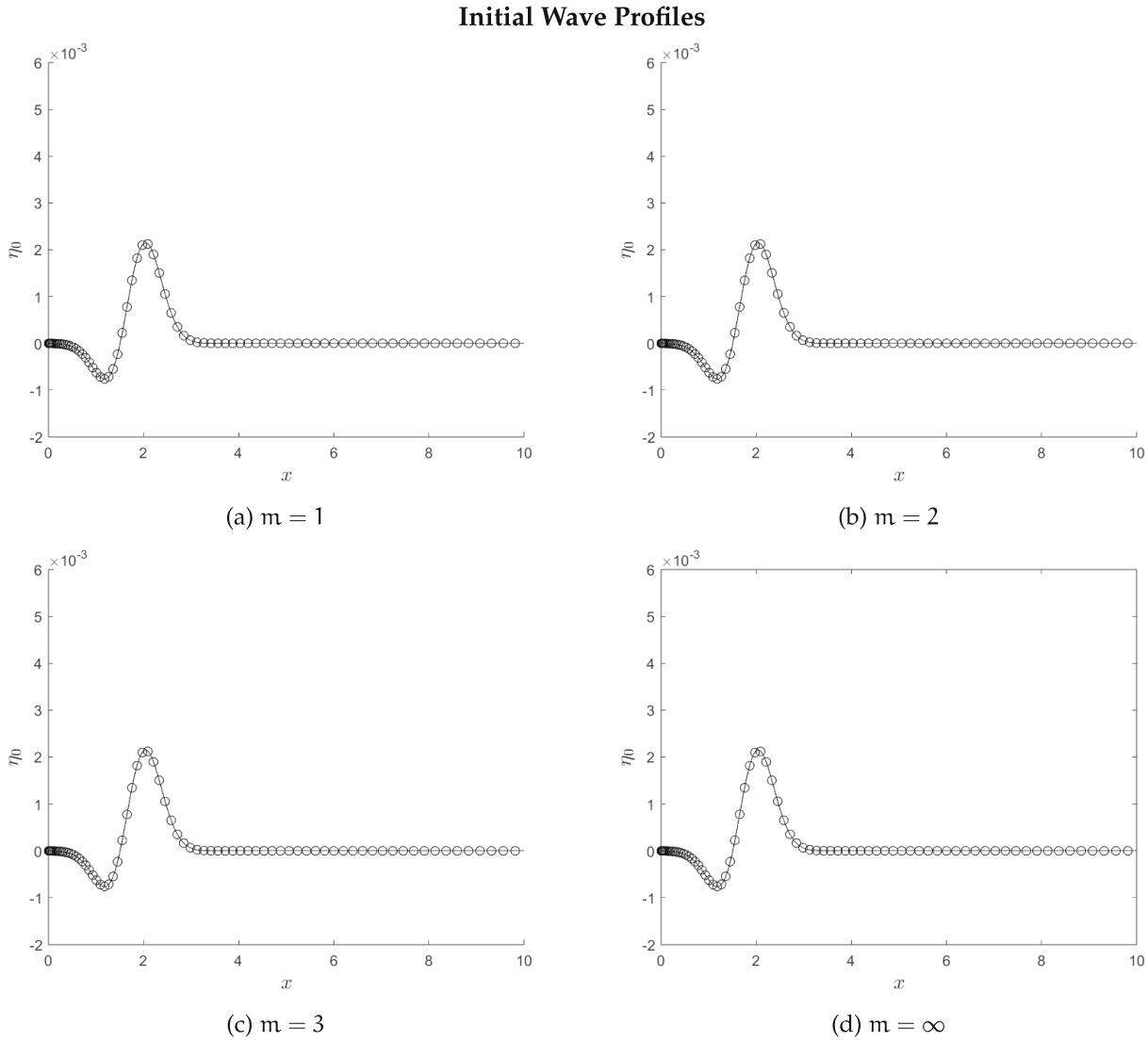

Fig. 2 A comparison of an initial displacement of an N-wave with the displacement predicted by our model for varying power-shaped bays. The solid black line gives the exact initial displacement and the open circles denote the initial displacement predicted by our model

Upon switching back to variable σ, one obtains [note that above r corresponds to ξ]

$$\psi_0(\sigma^2) = \frac{2\sqrt{\pi}\Gamma(1+1/m)}{\sigma^2\Gamma(1/m+1/2)} \int_0^{\sigma^2/\pi} \left(1-\left(\frac{\pi\xi}{\sigma^2}\right)^2\right)^{1/m-1/2} \psi(q\xi,0)\,\mathrm{d}\xi. \tag{4.15}$$

Now, denote

$$[\mathcal{A}_\alpha f(x)](s) = \int_0^s \frac{f(x)\,\mathrm{d}x}{(s^2-x^2)^\alpha} \tag{4.16}$$

as the singular Abel type integral of order α as seen in Deans (2007). After a straightforward substitution one obtains

$$\psi_0(\sigma^2) = \frac{2\Gamma\left(\frac{m+1}{m}\right)}{\Gamma\left(\frac{1}{m}+\frac{1}{2}\right)\sqrt{\pi}} \sigma^{-\frac{4}{m}} \left[\mathcal{A}_{1/2-1/m}\psi\left(\frac{qr}{\pi},0\right)\right](\sigma^2). \tag{4.17}$$

Now, we can use (4.17) to solve the inverse problem as follows: from the shoreline movement $x_0(t)$, we find $\psi(\tau,0) = -x_0(t) + \dot{x}_0(t)^2/2$ and $\tau = t - \dot{x}_0(t)$; after that, from (4.17), we find $\psi_0(\sigma)$, and finally, we find $\eta_0(x) = \psi_0(\sigma)$ and $x = \sigma - \eta_0(x)$. Note that the algorithm laid out above uses dimensionless units. The substitution (2.2) should be used when dealing with dimensional measurements.

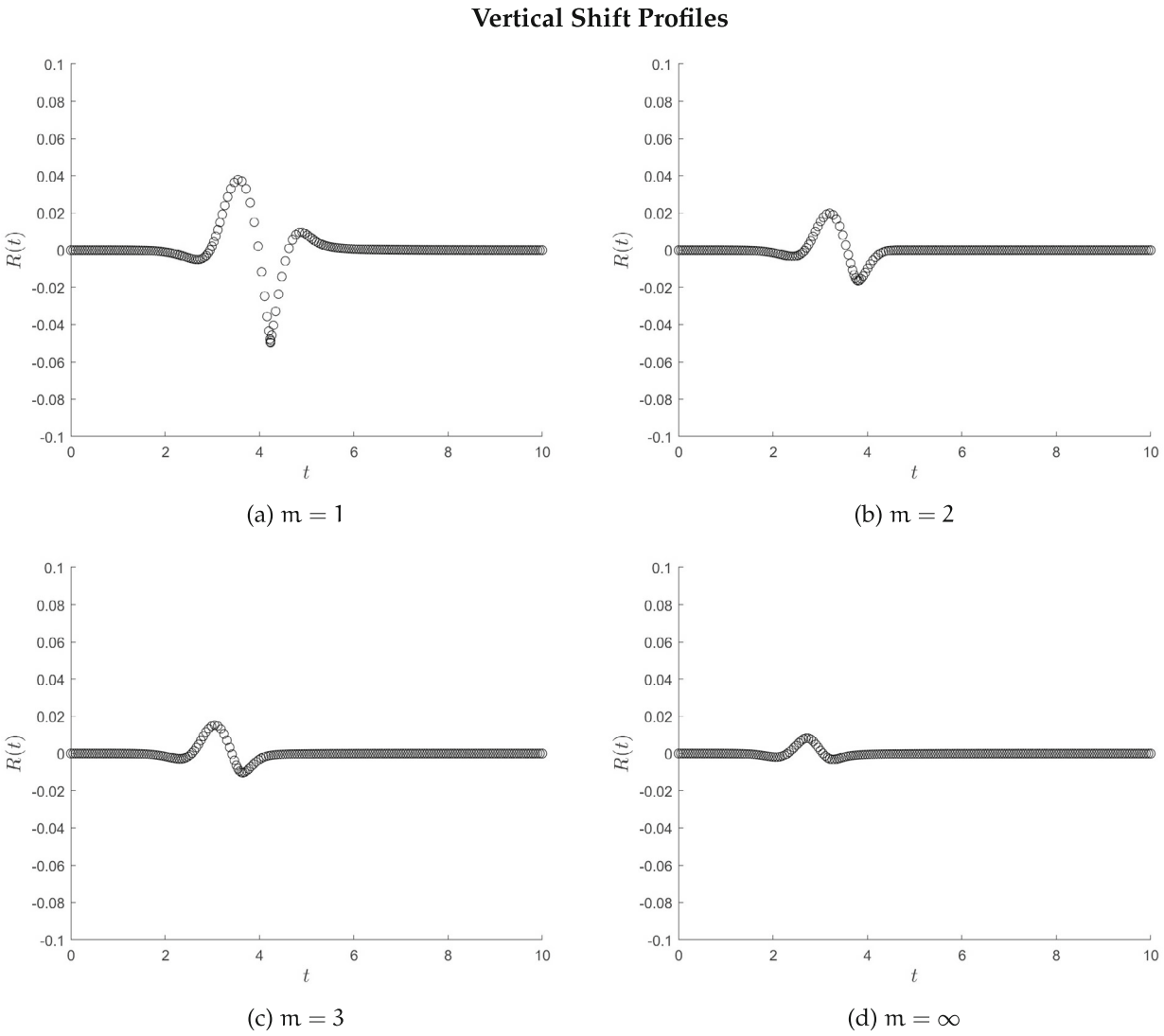

Fig. 3 Estimated vertical shift for an initial N-wave displacement corresponding to various bathymetries, where $R(t) = -x_0(t)/\alpha$, where $\alpha = 1$

Some remarks

The transform defined in (4.16) is in fact Erdélyi–Kober fractional integration operator (see for example Sneddon 1975). This operator is closely connected (Erdélyi 1970) to the Euler–Poisson–Darboux (EPD) equation, which one can obtain from SWE (2.1) by taking in the CG transform (3.1) $\sigma^2 = x + \eta(x, t)$. Moreover, one can use the CG transform used in Garayshin et al. (2016) to obtain the IBVP for the EPD equation, that solves the inverse problem, and after that use the technique laid out in Erdélyi (1970) to solve it. The only disadvantage of this approach is that it only applies for $m > 2$, while our method works for any positive m. In Erdélyi (1970), there is the claim that this restriction can be relaxed to any positive m; however, we have not investigated that.

It is worth noting that (4.16) has an inverse formula for $\alpha \in (0, 1)$ (Deans 2007), given as

$$\left[\mathcal{A}_\alpha^{-1} f(x)\right](s) = \frac{2\sin(\alpha\pi)}{\pi} \frac{\mathrm{d}}{\mathrm{d}s} \int_0^s \frac{x f(x)\,\mathrm{d}x}{(s^2 - x^2)^{1-\alpha}}. \tag{4.18}$$

Thus, for all $m > 2$, we can invert (4.17) to obtain (after substituting $s = \sigma^2$)

$$\psi(qr/\pi, 0) = \frac{\sqrt{\pi}}{\Gamma(1 + \frac{1}{m})\Gamma(\frac{1}{2} - \frac{1}{m})} \frac{\mathrm{d}}{\mathrm{d}r} \left[\mathcal{A}_{\frac{m+2}{2m}} s^{\frac{2}{m}} \psi_0(s)\right](r). \tag{4.19}$$

This allows to solve the direct problem using one integral operator, rather then composing two Fourier transform for $m > 2$.

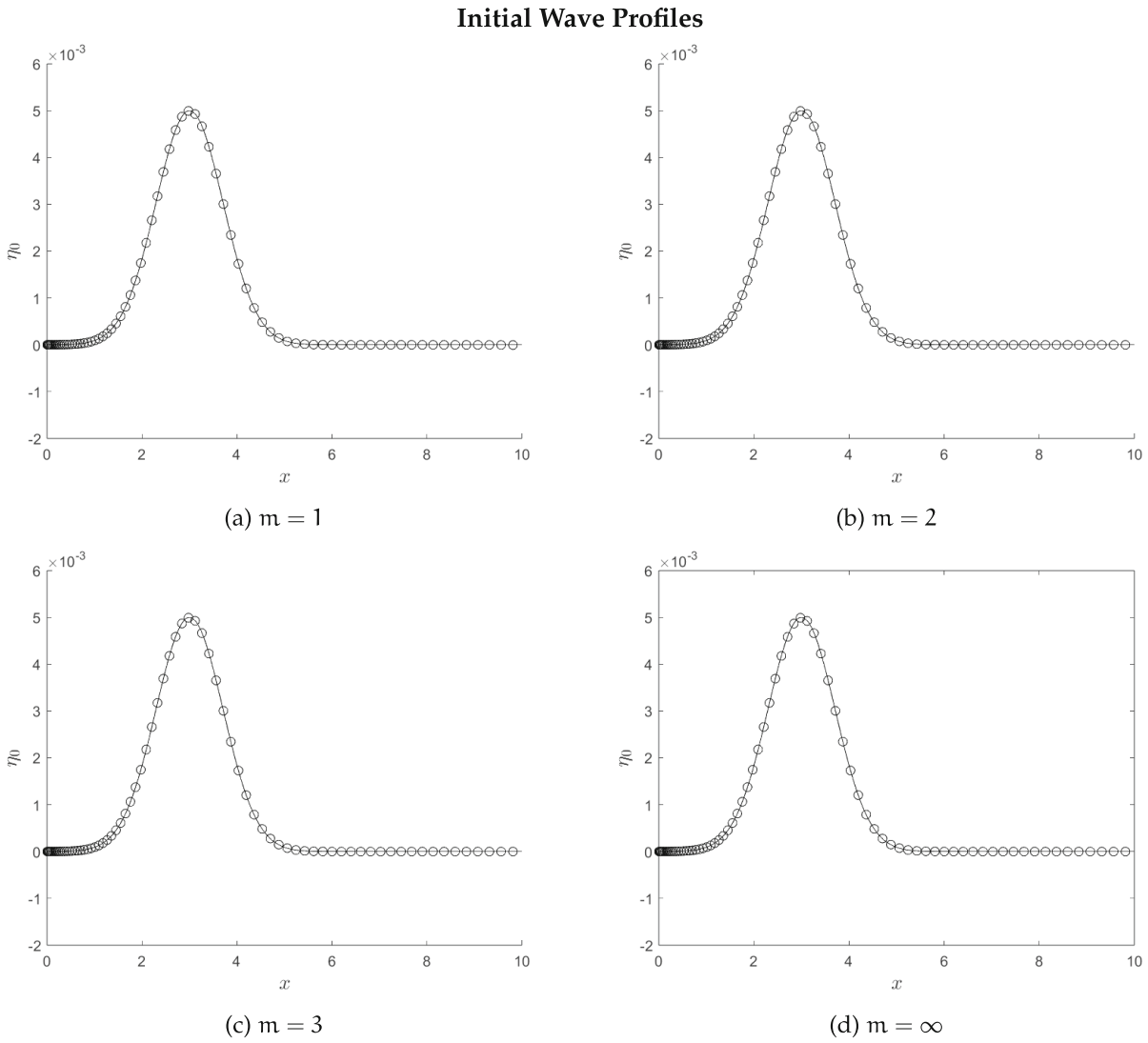

Fig. 4 A comparison of an initial displacement of an Gaussian wave with the displacement predicted by our model for varying power-shaped bays. The solid black line gives the exact initial displacement and the open circles denote the initial displacement predicted by our model

Particular cases

In the two most interesting cases, that is the case of the infinite plane beach corresponding to $m = \infty$ and a parabolic bay for $m = 2$, our solution can be shown to reduce down to particularly nice forms. For $m = \infty$, we have $q = 2\pi$ and so, (4.17) easily simplifies to

$$\psi_0(\sigma^2) = \frac{2}{\pi}\left[\mathcal{A}_{\frac{1}{2}}\psi(2r,0)\right](\sigma^2). \tag{4.20}$$

The substitution $\sigma' = \sigma^2$ and $\tau' = \tau/2$ turns (4.20) to the form obtained in Rybkin et al. (2023).

For $m = 2$, we have $q = \pi\sqrt{6}$, and so, (4.17) simplifies to

$$\psi_0(\sigma^2) = \frac{1}{\sigma^2}\left[\mathcal{A}_0\psi(\sqrt{6}r,0)\right](\sigma^2) = \frac{1}{\sigma^2}\int_0^{\sigma^2}\psi(\sqrt{6}r,0)\,\mathrm{d}r. \tag{4.21}$$

5 Estimate of the shape of the incoming wave

In this section, we give the exact lower bound for the support of the initial water displacement in terms of the shoreline data. First, we remind that for a scalar-valued function $f : X \to \mathbb{C}$, its support is the set $\operatorname{supp} f = \{x \in X | f(x) \neq 0\}$.

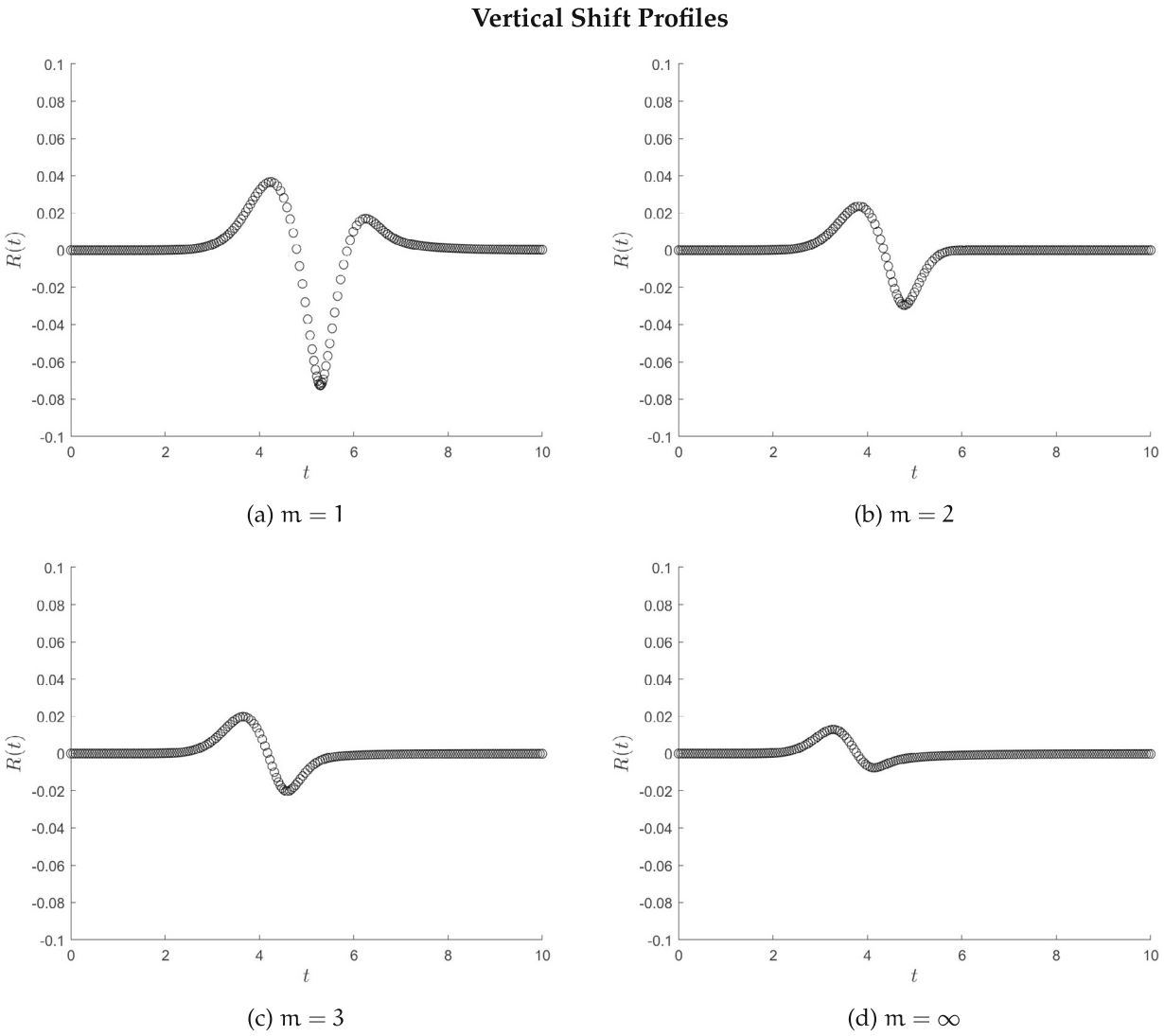

Fig. 5 Estimated vertical shift for an initial Gaussian wave displacement corresponding to various bathymetries, where $R(t) = -x_0(t)/\alpha$, where $\alpha = 1$

For the case $m = 2$, we have

$$\psi_0(\sigma^2) = \sigma^{-2} \int_0^{\sigma^2} \psi(\sqrt{6}r, 0)\, \mathrm{d}r, \tag{5.1}$$

and so, we deduce that $\inf \operatorname{supp} \psi_0(\sigma^2) = \inf \operatorname{supp} \psi \left(\sqrt{6}r, 0\right)$.

For $m > 2$, we can use Titchmarsh's convolution theorem, which states (see Titchmarsh 1926 for details) that if

$$(f * g)\Big|_{x\in(0,a)} = \left(\int_0^x f(t)g(x-t)\, \mathrm{d}t\right)\Big|_{x\in(0,a)} = 0, \tag{5.2}$$

and $g(x) > 0$ on $(0, a)$, then $f(x) = 0$ almost everywhere on $(0, a)$. From (4.19), we have

$$\psi\left(\frac{qr}{\pi}, 0\right) = C(m)\frac{\mathrm{d}}{\mathrm{d}r} \times \left(\int_0^r \left(\psi_0(s)s^{\frac{2}{m}}(r+s)^{\frac{2+m}{2m}}\right)(r-s)^{\frac{2+m}{2m}}\, \mathrm{d}s\right), \tag{5.3}$$

and so, we deduce that $\inf \operatorname{supp} \psi_0(s) \leq \inf \operatorname{supp} \psi \left(\frac{qr}{\pi}, 0\right)$. The inverse inequality immediately follows from (4.17), and so, combining these results, we obtain $\inf \operatorname{supp} \psi_0(s) = \inf \operatorname{supp} \psi \left(\frac{qr}{\pi}, 0\right)$.

Therefore, we can express the lower bound of the support of $\psi_0(\sigma)$. Since $\psi_0(\sigma) = \eta_0(x)$ and $\sigma = x + \eta_0(x)$, we can obtain the exact lower bound of the support $\eta_0(x)$, namely $\inf \operatorname{supp} \eta_0(x) = \inf \operatorname{supp} \psi_0(\sigma)$. In simple language

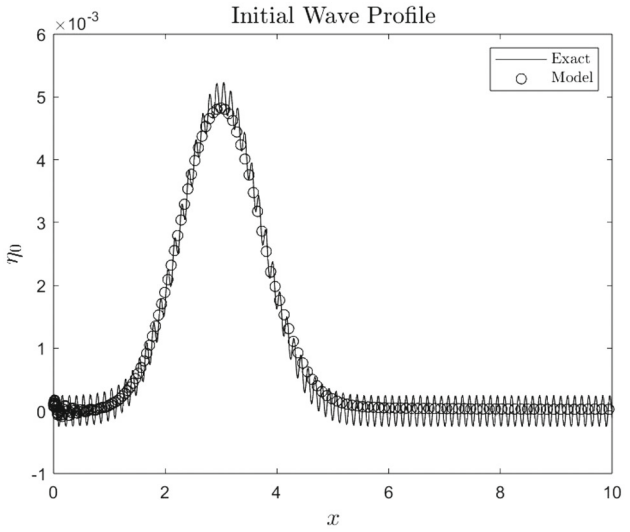

Fig. 6 Our model effectively cuts off any high-frequency waves, as can be seen with a Gaussian initial wave profile ($m = \infty$)

that means that we can express how far from the shore the displacement is at the time of an earthquake.

6 Numerical computations

In this section, we numerically verify our method for recovering η_0 in cases where $m \in \{1, 2, 3, +\infty\}$, that is for inclined parabolic bays of different shapes and an infinite sloping beach. In all of bathymetries, we consider an "N-wave"

$$\eta_0(x) = 2.5 \times 10^{-3} e^{-3.5(x-1.9625)^2} - 1.25 \times 10^{-3} e^{-3.5(x-1.4)^2}, \tag{6.1}$$

and a Gaussian wave

$$\eta_0(x) = 5 \times 10^{-3} e^{-(x-3)^2}, \tag{6.2}$$

with zero initial velocity. Existing code provided by Rybkin et al. (2021) was used to generate the shoreline data. We then implemented (4.20) and (4.21), respectively, to recover the initial displacements. Comparison of the exact initial wave profiles and those predicted by our model can be seen in Figs. 2 and 4. Corresponding shoreline movements can be seen in Figs. 3 and 5. It is worth noting that when we consider the same initial displacement for various bathymetries, the amplitude of the shoreline movement decreases as m increases.

It is common when a long tsunami wave is masked by wind waves that have higher frequency. Typically, the tsunami wave length is above 1 km, while wind waves have length of 90–180 ms. The integral transform we derived cuts off high-frequency oscillations. To demonstrate that we consider a

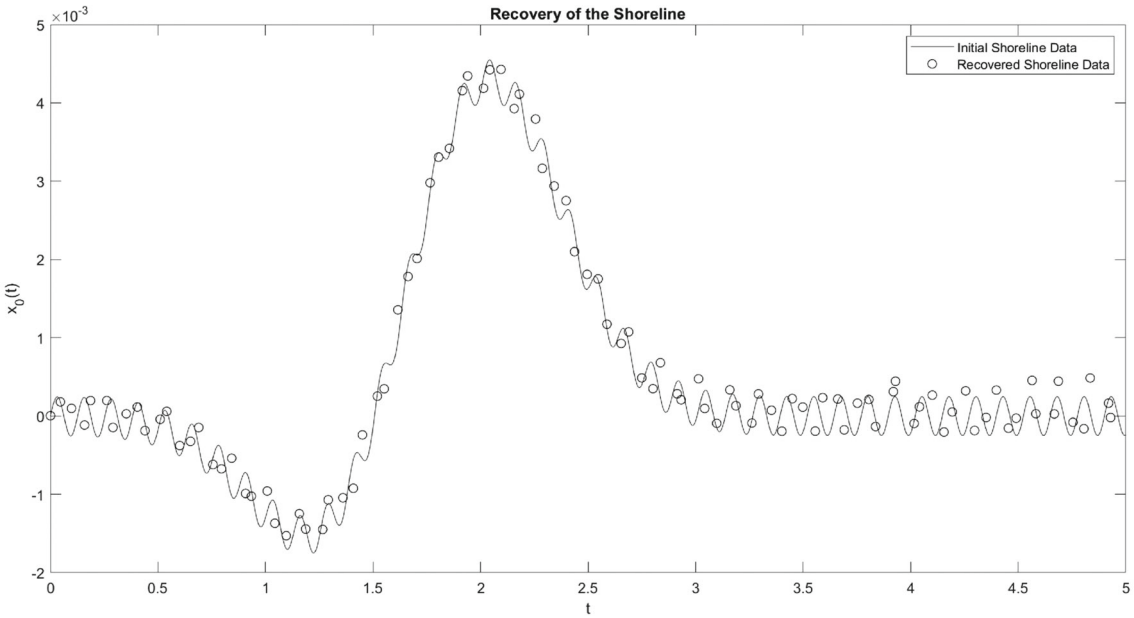

Fig. 7 While our numerical model does not remove noise found within the shoreline data, the model is able to cope with the existence of noise and recover its behaviour. In this case, our model begins by taking an analytical shoreline function with noise, given by $x_0(t) = 5\times10^{-3}e^{-3.5(t-1.9625)^2} - 2.5\times10^{-3}e^{-3.5(t-1.4)^2} + 2.5\times10^{-4}\sin(50t)$. This $x_0(t)$ is utilised to compute η_0 through the inverse problem. Subsequently, the model verifies the validity of this ensuring that the η_0 gained by recovering $x_0(t)$ through the direct problem directly matches the analytical $x_0(t)$ used to begin the computations (done in the case $m = 2$)

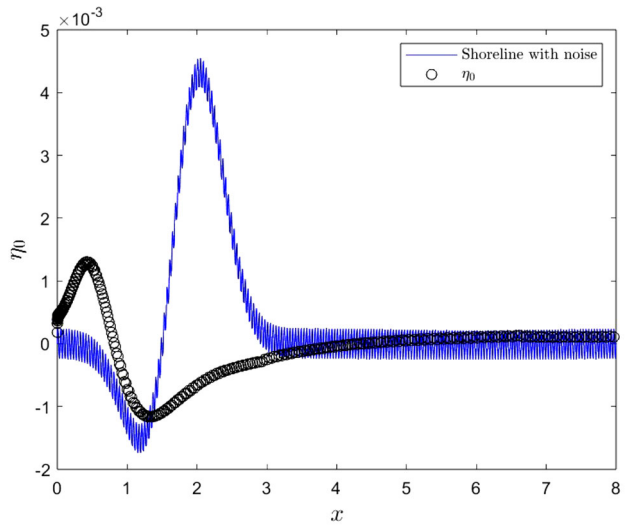

Fig. 8 The model appears to reduce high-frequency noise. Here, we took the shoreline to be $x_0(t) = 5 \times 10^{-3} e^{-3.5(t-1.9625)^2} - 2.5 \times 10^{-3} e^{-3.5(t-1.4)^2} + 2.5 \times 10^{-4} \pi \sin(50\pi t)$ and then computed η_0 using (4.20) which recovered a relatively smooth curve, as seen above

long wave with added disturbance

$$\eta_0(x) = 5 \times 10^{-3} e^{-(x-2)^2} + 2.5 \times 10^{-4} \sin(50x). \qquad (6.3)$$

Using the same methodology, we are again able to recover the initial wave profile (see Fig. 6) without the noise created by the high-frequency oscillations. While this is a coincidence of our numerical scheme, it holds practical significance. It suggests that our method can effectively reconstruct the long wave, presumably generated by the tsunami source, even in the presence of noise from common wind waves.

For analogous reasons, our model can handle noise in the shoreline data effectively (see Figs. 7 and 8). This capability may offer practical benefits, enhancing its robustness against noisy data collection at the shore.

It is worth noting that the noise reduction happens because of the numerical implementation of the integral. If one was able to compute the derived integral transform exactly, one would recover exact initial displacement with the noise.

7 Conclusions

We have put forth and solved an inverse problem for non-breaking tsunami waves in power-shaped bays assuming zero initial velocity. We have shown that for non-braking waves in power-shaped bathymetries, it is possible to recover the initial displacement of the water from the shoreline oscillations under the assumption of zero initial velocity.

Of course, the formulation of the problem is quite schematic from a practical standpoint: a one-dimensional problem, a bay with a constant slope, and a tsunami source relatively close to the coast. Nevertheless, this problem is part of the benchmarks for numerical tsunami models, and it is necessary for calculating possible scenarios to make predictive assessments of tsunami heights. To create tsunami hazard maps, calculations of potential tsunamis are currently being conducted using data from a synthetic earthquake catalogue, which includes approximately 100,000 events. Calculating such a large number of tsunamis from the source to the shore is too costly, so it is done in two stages: in the first stage, the characteristics of the tsunami are calculated up to depths of around 20–50 ms, and then, the wave height is recalculated at the shore using various versions of Green's law (Sorensen et al. 2012; Baptista et al. 2017; Basili et al. 2021). This is where the non-linear problem of wave run-up on the shore can serve as an effective means to improve estimates obtained through Green's law, and it was used, for example, in tsunami hazard assessments in the Sea of Japan (Choi et al. 2011). The formula for the run-up height of a solitary wave (Synolakis 1987) is especially often used. Refining the shape of the initial wave (and more generally, the initial flow velocity) in the run-up problem and assessing how critical it is for calculating run-up heights can be aided by solving the inverse problem.

While not considered here, we believe that a similar inverse problem can be treated in the case where the initial velocity is given as a function of the initial displacement, e.g., in the important case where $u_0 = -(2\sqrt{x+\eta_0} - 2\sqrt{x})$. Indeed, our preliminary results show this to be possible in the plane beach bathymetry. We hope to return to this case in a future work.

Our results here consider a tsunami wave with source an arbitrary distance from the shoreline. However, this is a highly idealised situation. In practice, dispersion can only be ignored when the wave is close to the shoreline. This suggests a more practical inverse problem where we have a finite bathymetry, that is $x \leq L$ for $L > 0$ and attempt to recover the wave at L. This is a boundary value problem and the techniques developed in Antuono and Brocchini (2007) and Rybkin et al. (2021) may be used to derive a shoreline equation. Finally, we note that our inversion method can be readily adjusted to the data read from a mareograph which is close to the shore. Indeed, using the angle of inclination, the mareograph readings can be converted into a displacement of the shoreline.

Acknowledgements This work was done as part of the 2023 summer REU program run by Dr. Alexei Rybkin and was supported by NSF grant DMS-2009980. Dr. Efim Pelinovsky thanks a support from RSF 22–17-00153. Oleksandr Bobrovnikov acknowledges support from Alaska EPSCoR NSF award #OIA-1757348 and DMS-2009980. The authors

also thank Dr. Ed Bueler for his valuable discussions of the problem with us. The authors also thank the UAF DMS for hosting us.

References

Abe K (1973) Tsunami and mechanism of great earthquakes. Phys Earth Planet Inter 7(2):143–153

Antuono M, Brocchini M (2007) The boundary value problem for the non-linear shallow water equations. Stud Appl Math 119:73–93

Aydin B (2020) On open boundary conditions for long wave equation in the hodograph plane. Stud Appl Math 384(13):7

Baptista MA, Miranda JM, Matias L, Omira R (2017) Synthetic tsunami waveform catalogs with kinematic constraints. Nat Hazards Earth Syst Sci 17:1253–1265

Basili R, Brizuela B, Herrero A, Iqbal S, Lorito S, Maesano FE, Murphy S, Perfetti P, Romano F, Scala A, Selva J, Taroni M, Thio HK, Tiberti MM, Tonini R, Volpe M, Glimsdal S, Harbitz CB, Løvholt F, Baptista MA, Carrilho F, Matias LM, Omira R, Babeyko A, Hoechner A, Gurbuz M, Pekcan O, Yalçner A, Canals M, Lastras G, Agalos A, Papadopoulos G, Triantafyllou I, Benchekroun S, Jaouadi KA, Abdallah SB, Bouallegue A, Hamdi H, Oueslati F, Amato A, Armigliato A, Behrens J, Davies G, Bucci DD, Dolce M, Geist E, Vida JMG, González M, Sánchez JM, Meletti C, Sozdinler CO, Pagani M, Parsons T, Polet J, Power W, Sørensen MB, Zaytsev A (2021) The making of the NEAM tsunami hazard model 2018 (NEAMTHM18). Front Earth Sci 8:616594

Carrier G, Greenspan H (1958) Water waves of finite amplitude on a sloping beach. J Fluid Mech 1:97–109

Carrier G, Wu T, Yeh H (2003) Tsunami run-up and draw-down on a plane beach. J Fluid Mech 475:79–99

Choi BH, Kaistrenko V, Kim KO, Min BI, Pelinovsky E (2011) Rapid forecasting of tsunami runup heights from 2D numerical simulation data. Nat Hazards Earth Syst Sci 11(3):707–714

Courant R, Hilbert D (1989) Methods of mathematical physics, vol 2. Wiley-VCH Verlag GmbH & Co

Deans S (2007) The radon transform and some of its applications. Dover books on mathematics series. Dover Publications

Didenkulova I, Pelinovsky E (2011) Non-linear wave evolution and runup in an inclined channel of a parbolic cross-section. Phys Fluids 23(8):086602

Didenkulova I, Pelinovsky E, Soomere T (2008) Run-up characteristics of tsunami waves of "unknown" shapes. Pure Appl Geophys 165:2249–2264

Dobrokhotov SY, Nazaikinskii V, Tolchennikov A (2017) Uniform asymptotics of the boundary values of the solution in a linear problem on the run-up of waves on a shallow beach. Math Notes 101:802–814

Erdélyi A (1970) On the Euler–Poisson–Darboux equation. J Anal Math 23:89–102

Fujii Y, Satake K, Sakai S, Shinohara M, Kanazawa T (2011) Tsunami source of the 2011 off the Pacific coast of Tohoku earthquake. Earth Planets Space 63:815–820

Garayshin V, Harris M, Nicolsky D, Pelinovsky E, Rybkin A (2016) An analytical and numerical study of long wave run-up in U-shaped and V-shaped bays. Appl Math Comp 297:187–197

Gradshteyn I, Ryzhik I (2007) Table of integrals, series, and products, 7th edn. Academic Press

Hartle H, Rybkin A, Pelinovsky E, Nicolsky D (2021) Robust computations of runup in inclined U- and V-shaped bays. Pure Appl Geophys 178:5017–5029

Kânoğlu U, Synolakis C (2006) Initial value problem solution of nonlinear shallow water-wave equations. Phys Rev Lett 97(14):148501

Levin B, Nosov M (2016) Physics of Tsunamis, 2nd edn. Springer

Løvholt F, Pedersen G, Bazin S, Kühn D, Bredesen R, Harbitz C (2012) Stochastic analysis of tsunami runup due to heterogeneous coseismic slip and dispersion. J Geophys Res 117

Nicolsky D, Pelinovsky E, Raz A, Rybkin A (2018) General initial value problem for the non-linear shallow water equations: runup of long waves on sloping beaches and bays. Phys Lett A 318(38):2738–2743

Okada Y (1985) Surface deformation due to shear and tensile faults in a half-space. Bull Seismol Soc America 75:1135–1154

Okada Y (1992) Internal deformation due to shear and tensile faults in a half-space. Bull Seismol Soc America 82:1018–1040

Pelinovsky E, Mazova R (1992) Exact analytical solutions of nonlinear problems of tsunami wave run-up on slopes with different profiles. Nat Hazards 6(3):227–249

Rybkin A (2019) Method for solving hyperbolic systems with initial data on non-characteristic manifolds with applications to the shallow water wave equations. Appl Math Lett 93:72–78

Rybkin A, Pelinovsky E, Didenkulova I (2014) Non-linear wave run-up in bays of arbitrary cross-section: generalization of the Carrier–Greenspan approach. J Fluid Mech 748:416–432

Rybkin A, Nicolsky D, Pelinovsky E, Buckel M (2021) The generalized Carrier–Greenspan transform for the shallow water system with arbitrary initial and boundary conditions. Water Waves 3:267–296

Rybkin A, Pelinovsky E, Palmer N (2023) Inverse problem for the nonlinear long wave runup on a plane sloping beach. Appl Math Lett 145:108786

Satake K (1987) Inversion of tsunami waveforms for the estimation of heterogeneous fault motion of large submarine earthquakes. J Geophys Res 94:5627–5636

Satake K (2022) Tsunamis, inverse problem of. In: Tilling RI (eds) Complexity in tsunamis, volcanoes, and their hazards. Encyclopedia of complexity and systems science series. Springer, New York, NY. https://doi.org/10.1007/978-1-0716-1705-2-570

Shimozono T (2016) Long wave propagation and run-up in converging bays. J Fluid Mech 798:457–484

Sneddon I (1975) The use in mathematical physics of Erdélyi–Kober operators and of some of their generalizations, vol 457. Lecture notes in mathematics. Springer

Sorensen MB, Spada M, Babeyko A, Wiemer S, Grunthal G (2012) Probabilistic tsunami hazard in the Mediterranean Sea. J Geophys Res Solid Earth 117:01305

Synolakis C (1987) The runup of solitary waves. J Fluid Mech 185:523–545

Synolakis C, Deb M, Skjelbreia J (1988) The anomalous behavior of the run-up of cnoidal waves. Phys Fluids 31:2–5

Tadepalli S, Synolakis C (1994) The runup of n-waves. Proc R Soc 445:99–112

Tinti S, Tonini R (2005) Analytical evolution of tsunamis induced by near-shore earthquakes on a constant-slope ocean. J Fluid Mech 535:33–64

Titchmarsh E (1926) The zeros of certain integral functions. Proc Lond Math Soc s2–25:283–302

Tuck E, Hwang L (1972) Long wave generation on a sloping beach. J Fluid Mech 51:449–461